parameters listed in Table I are taken from a previous work on $LnCp_2$ hydrides.[8b] Calculations on **6** and **7** have been carried out with and without inclusion of Lu 4f orbitals. As previously noted,[8b] these orbitals are only slightly perturbed by the ligand environment, always staying below the occupied π(Cp) levels. Thus, for computational time saving, they were not introduced in subsequent calculations.

When not specified in the text, the following bond distances (angstroms) and angles (deg) where used: Lu-H = 2.1; Lu-CH_3 = 2.6; Lu-C(Cp) = 2.85; C(Cp)-C(Cp) = 1.42; C-H = 1.09; Cp(centroid)-Lu-Cp(centroid) = 135; H-C-H = 109.47.

The variation of the total electronic energy of the considered systems during reactions 10, 11, 3, and 18 was obtained from an hypothetical reaction coordinate based on a linear transit between the geometries of the starting point and the assumed midpoint of the reaction followed by another linear transit between the midpoint and the final point of the reaction. In the starting and ending geometries, H-H and C-H distances of H_2 and CH_4 were, respectively, 0.74 and 1.09 Å and the following intermolecular contacts (angstroms) were considdered: Lu···H = 2.6; Lu···C = 3.05. A reasonable change in these distances does not affect significantly the general shape of the energy curve. The zero energy corresponds to the starting molecules at infinite separation in their stable conformation.

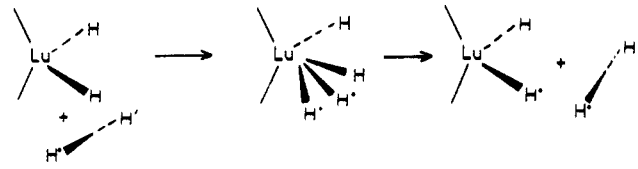

18

Acknowledgment. We thank Prof T. A. Albright for helpful discussions and Prof. T. J. Marks for providing results prior to publication.

(14) Hoffmann, R. *J. Chem. Phys.* **1963**, *39*, 1397. Hoffmann, R.; Lipscomb, W. N. *J. Chem. Phys.* **1962**, *36*, 2179; **1962**, *37*, 2872.
(15) Ammeter, J. H.; Bürgi, H.-B.; Thibeault, J. C.; Hoffmann, R. *J. Am. Chem. Soc.* **1978**, *100*, 3686.

Molecular Dynamics Simulation of a Small Calcium Complex in Aqueous Solution

Olle Teleman* and Peter Ahlström

Contribution from the Department of Physical Chemistry 2, Chemical Centre, University of Lund, POB 124, S-221 00 Lund, Sweden. *Received September 9, 1985*

Abstract: A molecular dynamics technique is used to simulate $CaEDTA^{2-}$ (two trajectories), H_4EDTA, and a calcium ion in aqueous solutions as well as pure water. The equation of motion is solved by means of a double time-step algorithm. The potential function allows for full intramolecular flexibility. The structure of "flexible" water resembles that of corresponding rigid water models, while dynamics seem slightly faster. This also applies to all dynamics of molecules dissolved in flexible water. The simulated coordination number of Ca^{2+} in a 0.45 M solution is 7. Comparison of the two $CaEDTA^{2-}$ trajectories indicates that quasiergodicity has been reached. In $CaEDTA^{2-}$ the calcium coordination number is also $\approx$7. Ligandation of calcium to the carboxyl groups is very strong, while the nitrogen-calcium relation is weaker. The structure of H_4EDTA is looser than that of $CaEDTA^{2-}$. Rotational correlation times for H_4EDTA are about half those of $CaEDTA^{2-}$, and the diffusion coefficient of H_4EDTA is about twice that of $CaEDTA^{2-}$. Both display some internal motion. Structural properties are plausibly reproduced, while dynamics seem fast. Results are compared to experimental data and discussed with respect to the properties of the potential.

Binding of calcium ions to different ligands is an important process in nature, where calcium ions frequently act as intracellular transmittor substances.[1] Many calcium-binding proteins with varying functions and binding constants ($K = 10^3$-10^8) are known.[1] Some proteins, e.g., calmodulins[2] and troponins,[3] work as regulators and undergo considerable conformational change on calcium binding. They often display a strong cooperativity that increases their sensitivity to changes in the calcium concentration. In other proteins, e.g., α-lactalbumin, the calcium ion is virtually permanently bound and appears to be a strongly connective structural element. In all of these proteins the calcium ion binds preferably to oxygen atoms in different amino acid residues, above all aspartic and glutamic acid.[1] The mechanisms of different processes involved in calcium binding is thus of great interest to molecular biology.

One way to obtain a deeper insight into the binding of calcium ions in proteins is to use computer simulation techniques. Recently we have embarked on such a study of the protein parvalbumin.[4] Such simulations however become rather complicated and very time-consuming. To provide a basis for their interpretation we have studied four smaller systems, namely pure water, one calcium ion in water, $CaEDTA^{2-}$ in water, and H_4EDTA in water. Pure water and calcium in water were mainly test systems for the model and the multiple time-step algorithm.[5] Comparison to experiment is possible since a wealth of X-ray and neutron diffraction data is available on the solvation of calcium ions, giving coordination numbers[6,7] and mean residence times[6] for the hydration shell of a calcium ion in water.

The $CaEDTA^{2-}$ complex is suitable as a test system for calcium binding because experimental data on both structure and dynamics

(1) Levine, B. A.; Williams, R. J. P. In *Calcium and Cell Function*; Cheung, W. W., Ed., Academic Press: London, 1982; pp 1-38.
(2) Perry, S. V. *Biochem. Soc. Trans.* **1979**, *7*, 593-617.
(3) Klee, C. B.; Crouch, T. H.; Richman, P. G. *Ann. Rev. Biochem.* **1980**, *49*, 489-515.
(4) Teleman, O.; Ahlström, P.; Jönsson, B. *Biophys. J.* **1985**, *47*, 399a.
(5) Teleman, O.; Jönsson, B. *J. Comput. Chem.* **1986**, *7*, 58-66.
(6) Friedman, H. L. *Chem. Scr.* **1985**, *25*, 42-48.
(7) Probst, M. M.; Radnai, T.; Heinzinger, K.; Bopp, P.; Rode, B. M. *J. Phys. Chem.* **1985**, *89*, 753-759.

0002-7863/86/1508-4333$01.50/0

Table I. σ_{ij} Parameters of the Lennard-Jones Potential (eq 2)[a]

	1	2	3	4	5	6	7	8
1	3.17	0.0	3.36	3.01	3.19	3.28	2.48	3.05
2		0.0	0.0	0.0	0.0	0.0	0.0	0.0
3			3.55	3.20	3.38	3.46	2.66	3.24
4				2.85	3.03	3.12	2.32	2.90
5					3.21	3.30	2.49	3.07
6						3.39	2.58	3.16
7							1.78	2.36
8								2.94

[a] Values are given in Å. The numbers 1–8 refer to the atom types, as given in Figure 1.

exist. The X-ray structure has been determined for both the Ca(CaEDTA)[8] and the Mg(MgEDTA)[9] complexes, thus providing two different starting configurations for a simulation. Diffusion coefficients[10] as well as NMR relaxation data[11] for the CaEDTA complex are available and give a possibility to study the dynamic properties of the model chosen. The main chelating groups in EDTA are carboxylate groups similar to most calcium-binding proteins. However, it is necessary to emphasize that the calcium binding of EDTA and of a protein differ in some respect, as in EDTA the interaction between the chelating groups and the calcium ion is the predominant energy contribution upon calcium binding, whereas in proteins the contribution to the potential energy from conformational changes may be equally important.[1]

Simulation Technique

Trajectories were generated by numerical integration of the Newtonian equation of motion, whereby all simulated systems were treated entirely as particle systems. The integration was performed by a fourth-order predictor-and-corrector algorithm, where the predictor is a standard Taylor expansion, and the corrector uses coefficients according to Gear.[12]

All intramolecular degrees of freedom were treated explicitly. The oscillation period of the faster vibrational modes amounts to $\approx 10^{-14}$ s and places a severe upper limit on the integration time step. To avoid any concomitant excessive demand on computer time a multiple time-step technique was used.[5] This amounts to a subdivision of any force into two components, one rapidly varying and one less so. The latter, which may then be evaluated less frequenly, is also the more time-consuming, and computing time reduces accordingly. In all cases the small time step, ∂t, used was $0.2 \cdot 10^{-15}$ s. The large time step, ∂T, was $1.2 \cdot 10^{-15}$ s, except where otherwise stated.

The temperature was calculated from the total kinetic energy, which is a straightforward procedure, since no constraints limit the number of degrees of freedom. All simulations were performed under periodic boundary conditions and formally in the microcanonical ensemble. Truncation of the interaction potential caused a numerical drift in the integration, amounting to 3.4% in the total energy in 5000 time steps (1 ps) for pure water. To remedy this, temperature scaling was applied, and the simulation ensemble is therefore in reality canonical. The pressure was calculated from the virial[13]

$$p = \frac{NkT}{V} - \frac{1}{3V}\sum_{i=1}^{N}[r_i \cdot \nabla_i U(r_1,...,r_N)] \qquad (1)$$

where N is the number of atoms, V the volume, $U(r_1,...,r_N)$ the potential (see below) and ∇_i the gradient with respect to the position of atom i.

The MD program used has been developed in our laboratory and is designed to generate fast code on a Cray 1A vector processor.[5] Uncertainties given represent one standard deviation, except where otherwise specified.

Potential

The functional form of the potential is given by eq 2 and 3. Equation 2 contains the noncovalent contributions, which are assumed to consist of a 6-12 Lennard-Jones potential[14] plus an electrostatic term where r_{ij} is the distance between two atoms i

$$U_{nc} = \begin{cases} \sum_{i<j} \left[4\epsilon_{ij}\left(\frac{\sigma_{ij}^{12}}{r_{ij}^{12}} - \frac{\sigma_{ij}^{6}}{r_{ij}^{6}}\right) + \frac{q_i q_j}{4\pi\epsilon\epsilon_0 r_{ij}}\right], r_{ij} < r_{cut} \\ 0, r_{ij} > r_{cut} \end{cases} \qquad (2)$$

and j. Partial charges q_i and q_j were taken from the literature[15,16] and were −0.82, +0.41, +2.0, −0.635, +0.27, −0.06, +0.05, and −0.12 of an elementary charge for atom types 1–8. For numbering of atom types, see Figure 1. For the Ca–EDTA complex the Lennard-Jones parameters ϵ_{ij} and σ_{ij} were calculated from the Kirkwood–Slater formula[17] and from the assumption that the Lennard-Jones potential minimum corresponds to the sum of the van der Waals radii of the two atoms. Data were taken from ref 18–20. A large variety of water models is available in the literature, see ref 20 and references therein. The simple point charge (SPC) model of Berendsen et al.[20] is parametrized according to eq 2 and was therefore used. The relative dielectric permittivity ϵ was assumed to be 1. Equation 2 is taken to describe not only intermolecular interactions but also those between atoms belonging to the same molecule but separated by at least three covalent bonds. A large value for r_{cut} is necessary to account for the long-ranged electrostatic term of equation 2.

The covalent contributions to the potential (equation 3) comprise harmonic terms in all covalent bond lengths and bond angles, as well as periodic terms in all dihedral angles

$$U_c = \sum_{\text{bonds}} A_i(r_i - r_{i,e})^2 + \sum_{\text{angles}} B_j(\alpha_j - \alpha_{j,e})^2 + \sum_{\text{dihedrals}} [C_{k,0} + \sum_{l=1}^{3} C_{k,l}\cos(l\beta_k)] \qquad (3)$$

where r_i is the actual length of the covalent bond i, $r_{i,e}$ the corresponding equilibrium length, α_j the actual value of the bond angle j, $\alpha_{j,e}$ the corresponding equilibrium value, and β_k the actual value of the dihedral angle k. Parameters B_i, $r_{i,e}$, A_j, $\alpha_{j,e}$, and $C_{k,l}$ were taken from the literature.[19–22] While Reimers and Watts[23,24]

(8) Barnett, B. L.; Uchtman, V. A. *Inorg. Chem.* **1979**, *18*, 2674–2678.
(9) Passer, E.; White, J. G.; Cheng, K. L. *Inorg. Chim. Acta* **1977**, *24*, 13–23.
(10) Mateo, P. L.; Hurtado, G. G.; Vidal-Abarca, J. B. *J. Phys. Chem.* **1977**, *81*, 2032–2034.
(11) Drakenberg, T. *Acta. Chem. Scand., Ser.* **1982**, *A36*, 79–82.
(12) Gear, C. W. *Numerical Initial Value Problems in Ordinary Differential Equations*; Prentice Hall: Englewood Cliffs, NJ, 1971; pp 148–154.
(13) Hansen, J. P.; MacDonald, I. R. *Theory of Simple Liquids*; Academic Press: London, 1976; pp 19–21.
(14) Lennard-Jones, J. E. *Proc. Roy. Soc. London A* **1924**, *106*, 463–477.
(15) McCammon, J. A.; Wolynes, P. G.; Karplus, M. *Biochemistry* **1979**, *18*, 927–942.
(16) Hermans, J.; Berendsen, H. J. C.; v. Gunsteren, W. F.; Postma, J. P. M. *Biopolymers* **1984**, *23*, 1513–1518.
(17) Slater, J. C.; Kirkwood, J. G. *Phys. Rev.* **1931**, *37*, 682.
(18) Margenau, H.; Kestner, N. R. *Theory of Intermolecular Forces*; Pergamon Press: New York, 1969.
(19) v. Gunsteren, W. F.; Karplus, M. *Macromolecules* **1982**, *15*, 1528–1544.
(20) Berendsen, H. J. C.; Postma, J. P. M.; v. Gunsteren, W. F.; Hermans, J. In *Intermolecular Forces*; Pullman, B., Ed.; D. Reidel: Dordrecht, 1981; pp 331–342.

Table II. ϵ_{ij} Parameters of the Lennard-Jones Potential (eq 2)[a]

	1	2	3	4	5	6	7	8
1	0.638	0.0	0.060	1.28	0.719	0.703	0.873	0.801
2		0.0	0.0	0.0	0.0	0.0	0.0	0.0
3			0.009	0.107	0.061	0.063	0.065	0.071
4				2.70	1.48	1.42	2.00	1.63
5					0.824	0.801	1.01	0.897
6						0.783	0.933	0.875
7							2.09	1.17
8								0.998

[a] Values are given in kJ·mol^{-1}. Numbers 1–8 refer to the atom types, as given in Figure 1.

Table III. Covalent Potential Parameters (eq 3)[a]

bonds	r_e	B
1–2	1.00	2318.
4–5	1.22	1883.
5–6	1.52	1674.
6–7	1.03	1912.
6–8	1.46	1883.
bond angles	α_e	A
2–1–2	109.47	58.33
4–5–4	129.0	63.73
4–5–6	115.9	50.99
5–6–7	109.5	60.92
5–6–8	110.5	114.72
6–6–7	109.5	60.92
6–6–8	109.6	63.73
7–6–7	109.5	60.92
7–6–8	109.5	60.92
6–8–6	108.9	89.22
dihedral angles	C_1	C_2	C_3
4–5–6–7	0.0	0.0	0.0
4–5–6–8	0.0	0.0	0.42
7–6–6–7	0.0	0.0	0.0
7–6–6–8	0.0	0.0	0.0
8–6–6–8	0.0	0.0	2.09
5–6–8–6	0.0	0.0	−1.26
7–6–8–6	0.0	0.0	0.0

[a] Values of r_e are given in Å, those of B in kJ·mol^{-1}·Å^{-2}, those of α_e in deg, those of A in J·mol^{-1}·deg^{-2} and those of C_{1-3} in kJ·mol^{-1}. Numbers 1–8 refer to the atom types, as defined by Figure 1.

have shown that inclusion of anharmonicity into the intramolecular potential is necessary in order to reproduce the water infrared spectrum satisfactorily, we do not expect the anharmonicity terms to affect intermolecular couplings very dramatically. As this work is not aimed at a detailed investigation of high frequency vibrations, the potential parametrization of eq 3 was assumed to be adequate. Also the hydrogen atoms within the EDTA molecule were treated explicitly. As no more than 12 nonpolar hydrogen atoms are present in any simulation, this does not increase computing time significantly. All potential parameters used are given in Tables I–III.

The parameters of the SPC model describe effective interactions of rigid water molecules as obtained from a fit to thermodynamic data.[20] The model thus includes, in an average way, any effects of intramolecular motion. In the present approach molecular flexibility was added without adjustment of the noncovalent interaction parameters. In consequence they cannot be relied on to represent an optimal fit to the above-mentioned data. However, the inclusion of all intramolecular flexibility is computationally advantageous, since use of constraints is detrimental to the vectorization properties of the program. It has not yet been clarified whether an exact quantum mechanical treatment is best approximated by a rigid, classical or by a flexible, classical model.

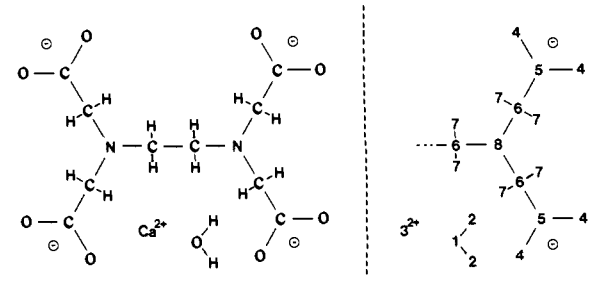

Figure 1. The EDTA^{4-} molecule, the Ca^{2+} ion, and one water molecule. Figures designate the atom types. All atoms of the same type are assumed to have identical interaction parameters, see Tables I–III.

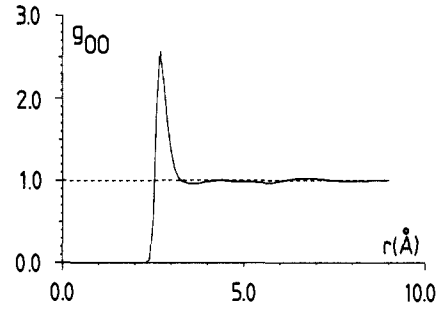

Figure 2. Radial distribution function for the oxygen–oxygen distances obtained from the simulation of pure water.

This further motivates investigation of the latter approach.

Results and Discussion

Pure water was simulated in the form of 216 water molecules enclosed in a cubic box with a side length of 18.6 Å. The cutoff distance for noncovalent interactions (r_{cut}) was set to 8.5 Å. The initial system was a primitive cubic lattice with random molecular orientations. Simulation parameters are summarized in Table IV.

The temperature was set to 300 K. Temperature drift and scaling intervals were such that the average temperature increased to 301 ± 1 K. Thermodynamic simulation data are given in Table IV. The average total potential energy was −40.2 ± 0.2 kJ/mol, whereas for rigid SPC water the potential energy amounts to −42.2 kJ/mol.[20] Our value includes however the potential energy of the three intramolecular degrees of freedom. Correction by 1.5 kT (= 3.76 kJ/mol) gives −43.9 kJ/mol. Reimers and Watts[23] give a value of −1.0 kJ/mol for the change in the water dimer potential minimum on inclusion of intramolecular flexibility. Many particle effects and the inoptimality of potential parameters contribute to the remaining difference and to the difference between our value and the experimental one (−41.64 kJ/mol, cf. Table III, p 181 of ref 25). That the atomic charges in a molecule change on geometric rearrangement[26] is one example of neglected many particle effects, others will be discussed below.

The bond length contribution to the potential energy, i.e., that arising from the first term of eq 3, was found to be ≈0.47 kT per

(21) Dolphin, D.; Wick, A. E. *Tabulation of Infrared Spectral Data*; Wiley Interscience: New York, 1977.
(22) Herzberg, G. *Molecular Spectra and Molecular Structure: Infrared and Raman Spectra of Polyatomic Molecules*; van Nostrand: Princeton, 1945.
(23) Reimers, J. R.; Watts, R. O. *Chem. Phys.* **1984**, *85*, 83–112.
(24) Reimers, J. R.; Watts, R. O. *Chem. Phys.* **1984**, *91*, 201–223.
(25) Postma, J. P. M. University of Groningen, 1984, Ph.D. Dissertation, *A Molecular Dynamics Study of Water.*
(26) John, I. G.; Bacskay, G. B.; Hush, N. S. *Chem. Phys.* **1980**, *51*, 49–60.

Table IV. Simulation Parameters and Thermodynamic Averages[a]

	water	calcium	"C"	"M"	"H"
length of box side (Å)	18.6	15.5	21.7	21.7	21.7
potentl cutoff dist (Å)	8.5	7.5	10.0	10.0	10.0
equilbrtn (ps)	31.3	24.6	16.93	18.56	7.68
length of trajctry (ps)	57.6	40.0	46.08	46.08	46.08
sampling intrvl (ps)	0.096	0.100	0.096	0.096	0.096
no. of neighbor prs in thousands	83	32.6	194	197	195
cray 1A cpu t (h)	3.01	0.61	5.10	5.18	4.42
cpu per pr intrctn (μs)	2.72	3.37	2.47	2.46	2.12[b]
temp (K)	301 ± 1	311 ± 2	303 ± 1	303 ± 1	302 ± 1
press. (kbar)	1.71 ± 0.2	2.02 ± 0.18	1.68 ± 0.33	1.66 ± 0.37	1.55 ± 0.22
potntl energy (MJ/mol)	−8.67 ± 0.05	−6.18 ± 0.03	−15.29 ± 0.07	−15.49 ± 0.07	−12.89 ± 0.07
noncovlnt energy (MJ/mol)	−9.78 ± 0.06	−6.72 ± 0.04	−16.87 ± 0.08	−17.10 ± 0.08	−14.54 ± 0.07
bond energy (MJ/mol)	0.51 ± 0.01	0.20 ± 0.01	0.60 ± 0.01	0.61 ± 0.01	0.68 ± 0.01
bond angle energy (MJ/mol)	0.60 ± 0.01	0.34 ± 0.01	0.97 ± 0.03	0.98 ± 0.03	0.95 ± 0.02
dihedral angle energy (MJ/mol)	0.	0.	0.01 ± 0.003	0.01 ± 0.001	0.01 ± 0.002

[a] Energies are given in MJ per mol of systems. "Potential energy" refers to the total potential energy and is the sum of "noncovalent", "bond", "bond angle", and "dihedral angle" energies, cf. eq 2 and 3. [b] At the time of the "H" simulation a new compiler had been installed, cutting computing time by some 13%.

degree of freedom, very close to the equipartition value. The contribution to potential energy due to bond angles (second term of eq 3) amounts to 1.12 kT per degree of freedom, which indicates that the angle bending is more strongly coupled to the intermolecular degrees of freedom.

The radial distribution function $g_{OO}(r)$ for the oxygen to oxygen distances is given in Figure 2. It contains a nearest-neighbor peak at 2.7 Å with a peak intensity of 2.6 as well as resolved second and third layers at 4.4 and ≈6.7 Å, respectively, and thus largely resembles that of rigid SPC water molecules.[20] This applies also to the $g_{OH}(r)$ and $g_{HH}(r)$ radial distribution functions.[25] All three $g(r)$ functions also resemble their counterparts obtained for the Matsuoka–Clementi–Yoshimine (MCY)[27] water model,[28,29] whereas their secondary structure is somewhat less pronounced than for the two rigid water molecule models. Reimers and Watts[24] observed an increased structure in all three $g(r)$ functions on inclusion of intramolecular flexibility. We cannot reconcile these data with ours as yet. However, it should be noted that $g_{OO}(r)$ for the rigid RWK2[24] model lacks all secondary structure, whereas that of $g_{OO}(r)$ for rigid SPC water is comparable to that derived from experimental data.[30] This issue will be further addressed in a forthcoming article. Integration of the first peak in $g_{OO}(r)$ gives a number of nearest neighbors of about four, integration of that of $g_{OH}(r)$ indicates that each water molecule engages in about four hydrogen bonds.

The diffusion coefficient, D, was calculated from eq 4

$$D = \lim_{t\to\infty} \frac{1}{6t} \langle |r_i(0) - r_i(t)|^2 \rangle_i \qquad (4)$$

where t is the time and $r_i(t)$ the position of atom i and the average runs over all atoms. To obtain a measure of the uncertainty in D the trajectory was divided into three parts, each covering 19.2 ps, and a value of D was calculated from each of them (D_1, D_2, D_3). The uncertainty, d, was then estimated by $|D_{max} - D_{min}|$, where D_{max} is the largest and D_{min} the smallest of the D_i's (i = 1, 2, 3). The diffusion coefficient was found to be 6.2 ± 0.5·10^{-9} m^2/s. While larger than the experimental value (2.37·10^{-9} m^2/s, see ref 31), it is still inside the range of diffusion coefficients reported for rigid SPC water.[32] For pure water an uncertainty can also be obtained by dividing the system into subsystems and analyzing these separately, thus providing a basis for standard statistical analysis. The uncertainty then amounts to 0.4·10^{-9} m^2/s. This technique however is not applicable to systems that contain only one molecule of the investigated species, such as the EDTA systems, and we have chosen to use the former recipe throughout.

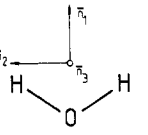

Figure 3. Unit vectors of a perpendicular, molecular coordinate system for water.

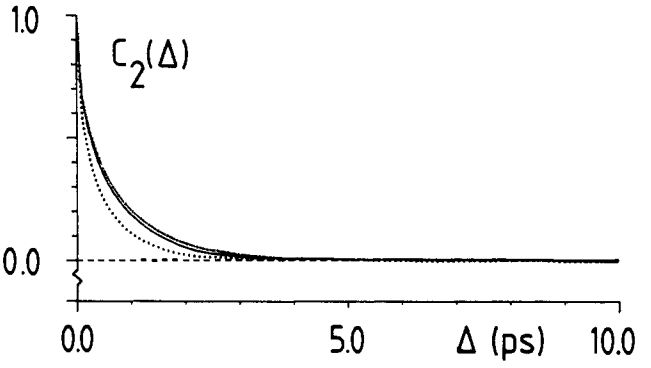

Figure 4. Second-order time correlation functions, $C_2(\Delta)$, for molecular vectors of water, as defined in Figure 3. Solid line refers to n_1, dot-dashed to n_2, and dotted to n_3.

Reorientational autocorrelation functions for a vector n were calculated as

$$C_j(\Delta) = \frac{1}{N} \sum_{i=1}^{N} \langle P_j(\cos \theta_i(t,\Delta)) \rangle_t \qquad (5)$$

where $\theta_i(t,\Delta)$ is the angle between $n(t + \Delta)$ and $n(t)$, P_j is the Legendre polynomial of order j, the brackets indicate a time average, and the summation runs over all water molecules. Below, the $C_j(\Delta)$ will be referred to as the jth order time correlation function (tcf). Figure 3 depicts the used vectors; one along the dipole moment of the water molecule, one in the plane of the molecule but perpendicular to the first, and lastly one perpendicular to the other two. $C_2(\Delta)$ for these three vectors is shown in Figure 4. These functions contain a rapid component, the decay of which is complete within ≈0.2 ps and which reduces the magnitude of $C_2(\Delta)$ by 30–40%. This has been found in other simulations of liquid water and is usually interpreted as due to a hindered rotational motion of the water molecule.[29] After 0.2 ps, $C_2(\Delta)$ can be very closely approximated with an exponential, which was obtained from a fit between 0.5 and 2.0 ps. The correlation time, τ_{2e}, corresponding to this exponential is given

(27) Matsuoka, O.; Clementi, E.; Yoshimine, M. *J. Chem. Phys.* **1976**, *64*, 1351–1361.
(28) Impey, R. W.; Klein, M. L.; McDonald, I. R. *J. Chem. Phys.* **1981**, *74*, 647–652.
(29) Impey, R. W.; Madden, P. A.; McDonald, I. R. *Mol. Phys.* **1982**, *46*, 513–539.
(30) Narten, A. H. *J. Chem. Phys.* **1972**, *56*, 5681–5687. Narten, A. H.; Danford, M. D.; Levy, H. A. *Discuss Faraday Soc.* **1967**, *43*, 97–107. Narten, A. H.; Levy, H. A. *J. Chem. Phys.* **1971**, *55*, 2263–2269.
(31) Krynicki, K.; Green, C. D.; Sawyer, D. W. *Discuss Faraday Soc.* **1978**, *66*, 199–208.
(32) Postma, J. P. M.; Berendsen, H. J. C.; Haak, J. R. *Symp. Faraday Soc.* **1983**, *17/9*, 1A–7A.

Table V. Correlation Times, τ_2, for Water[a]

		this work	rigid SPC	MCY	exprmtl
n_1,	long times	0.79	1.5	1.36	
	integral	0.56	1.06	0.78	
n_2,	long times	0.89	1.8	2.04	
	integral	0.63	1.27	1.48	2.06
n_3,	long times	0.63		1.34	
	integral	0.44		0.76	

[a] All values in ps. The values for "long times" have, in all cases, been obtained by fitting an exponential from 0.5 to 2.0 ps. "Integral" values have been corrected for the initial rapidly decaying component and correspond to the integral of the entire tcf. The values for rigid SPC are from ref 25, but the integral correction was applied by us and is the same as that for flexible SPC water. MCY values are from ref 28 and the experimental ones from ref 33. The simulation temperature was 301.3 K, and all other values have been experimentally interpolated to that temperature.

in Table V under the denomination "long times". The integral of the entire correlation function defines the full correlation time, also given in Table V, and was calculated as (Δ in ps)

$$\tau_2 = \int_0^{0.5} C_2(\Delta)\, d\Delta + C_2(0.5)\tau_{2e} \qquad (6)$$

where the integral from 0 to 0.5 ps was evaluated numerically. A comparison to MD simulation results on rigid SPC water,[25] and MCY water[28] as well as with experimental data[33] is made in Table V. The reorientational correlation times of the flexible SPC water are smaller than those of rigid SPC water and rigid MCY water by approximately a factor of two. On the other hand, the differences between the vectors n_1, n_2, and n_3 are qualitatively the same. Compared to experimental data,[33] the correlation time, τ_2, for n_2 of the flexible SPC water is smaller by a factor of three.

The simulated diffusion coefficient and reorientation times are consistent and describe a water molecule that is too mobile. It is clear that, while correctly representing the thermodynamic properties of water, it is less accurate in reproducing dynamic properties.

From experimental data on D ($2.37 \cdot 10^{-9}$ m^2/s, ref 31) and τ_2 (2.06 ps, ref 33) and the simulation results reported in this work, we note that these two properties scale in about the same way. It is thus tempting to see how well they can be accommodated within a hydrodynamic model. An effective radius may be calculated from the Stokes–Einstein formulae (eq 7)[34]

$$D = \frac{kT}{6\pi\eta r_{e,D}} \qquad \tau_2 = \frac{8\pi\eta r_{e,\tau}^3}{6kT} \qquad (7)$$

where k is the Boltzmann constant and η the viscosity. The effective radius, $r_{e,D}$ or $r_{e,\tau}$, is the radius of the hypothetical, spherical molecule that would have the same value of the dynamic entity (D or τ_2) as the actual one. With the experimental values of D, τ_2, and η ($0.865 \cdot 10^{-3}$ kg/ms) one finds $r_{e,D} = 1.08$ and $r_{e,\tau} = 1.33$ Å. The latter is larger by ≈24%, giving a measure of the accuracy with which the hydrodynamical model can be considered to describe real water. If we assume that $r_{e,D} = r_{e,\tau}$, we can insert the simulated values of D and τ_2 into eq 7 in order to obtain an effective radius

$$r_{\text{eff}} = 3[0.5\tau_2 D]^{0.5} \qquad (8)$$

and a viscosity

$$\eta = \frac{kT}{18\pi D}[0.5\tau_2 D]^{-0.5} \qquad (9)$$

Equations 8 and 9 now yield $r_{\text{eff}} = 1.3 \pm 0.4$ Å and $\eta = 0.27 \pm 0.07 \cdot 10^{-3}$ kg/ms, respectively.

One Calcium Ion in Water. In order to obtain a picture of the hydration properties of a calcium ion as described by our potential,

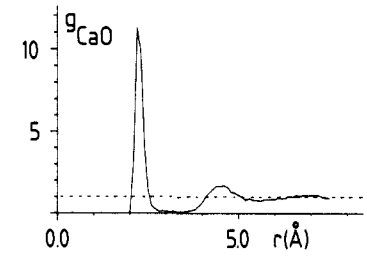

Figure 5. Radial distribution function for calcium–oxygen distances obtained from the simulation of Ca^{2+} in water.

one Ca^{2+} ion and 124 water molecules were simulated. The system was enclosed in a cubic box with a side length of 15.5 Å. Initially, the calcium was placed at the center of the box, and the water molecules were centered on the bases of a primitive cubic lattice, with their orientations randomized. Simulation parameters are given in Table IV.

The large time step was $2 \cdot 10^{-15}$ s. The temperature was set to 300 K, and the average temperature was 311.3 K. The short cutoff radius and the ionic nature of the system cause this large temperature drift. Thermodynamic averages are given in Table IV.

The radial distribution function $g_{Ca-O}(r)$ for the distances between the calcium ion and all water oxygens is shown in Figure 5 and contains two well-resolved neighbor layers. That of nearest neighbors is centered at 2.30 ± 0.14 Å, and integration yields a coordination number of 7.0 ± 0.2. Probst et al.[7] have obtained a value of ≈9 for the calcium ion coordination number from MD simulations of $CaCl_2$ in water by using a three-body, central force potential.[35,36] From X-ray diffraction data however they find a value of ≈7, in agreement with our results. The next layer contains about 20 water molecules at an average distance of 4.8 Å. The nearest-neighbor peak in $g_{Ca-H}(r)$ contains 14.3 ± 0.4 hydrogens and is situated at 3.0 ± 0.2 Å. In order to characterize the structure of the first hydration shell, we have employed the angular probability density $Q(\theta,\varphi)$, where θ and φ are the polar angles of the water dipole vector with respect to an axis defined by the vector from the calcium ion to the oxygen atom of the water molecule. Due to the symmetry we can integrate over the azimuth, φ, to obtain $Q(\theta)$. The distribution of θ angles, $P(\theta)$, is now obtained as $Q(\theta)$ multiplied by the volume element, i.e., proportional to $Q(\theta) \sin\theta$. One finds an average of $\langle\theta\rangle = 20° \pm 11°$, whereas $Q(\theta)$ has a narrow maximum at 0°. The orientation distribution of liganded waters is thus, naturally enough, strongly polarized by the calcium ion. From neutron diffraction measurements, Hewish et al.[37] obtain a mean angle of 38° ± 9° for a 1 *m* $CaCl_2$ solution. The Ca^{2+} coordination number is given as 10.0 ± 0.6, which deviates by 3 from our findings. They also find the coordination number to be strongly increasing with decreasing concentration. As the simulated solution had a molality of 0.45, this increases the difference in coordination number and also makes a direct comparison to our results on the tilt angle difficult. Data are available also on $NiCl_2$ solutions,[38] and a mean tilt angle of 17° ± 10° is given for a 0.46 *m* solution, where also the cation coordination number, reported to be 6.8 ± 0.8, is very close to our simulation value.

The diffusion coefficients of the calcium ion were obtained from the slope of the mean square displacement and were found to be $2.7 \pm 0.4 \cdot 10^{-9}$ m^2/s. Mateo et al.[10] give an experimental value of $0.91 \cdot 10^{-9}$ m^2/s at 308 K, which corresponds to $0.97 \cdot 10^{-9}$ m^2/s at 311 K. Our simulation value is larger by a factor of ≈2.8, which is very close to the ratio between simulation and experimental values of the water self-diffusion coefficient. The correlation

(33) Jonas, J.; DeFries, T.; Wilbur, D. J. *J. Chem. Phys.* **1976**, *65*, 582–588.
(34) Marshall, A. G. *Biophysical Chemistry; Principles, Techniques and Applications*; Wiley: New York, 1978; pp 712–715.
(35) Bopp, P.; Jancso, G.; Heinzinger, K. *Chem. Phys. Lett.* **1983**, *98*, 129–133.
(36) Jancso, G.; Bopp, P. *Z. Naturforsch., A: Phys., Phys. Chem. Kosmophys.* **1983**, *38A*, 206–213.
(37) Hewish, N. A.; Neilson, G. N.; Enderby, J. E. *Nature (London)* **1982**, *297*, 138–139.
(38) Neilson, G. W.; Enderby, J. E. In *Water, A Comprehensive Treatise*; Franks, F., Ed.; Plenum Press: New York, 1979, Vol. 6, pp 1–46.

function $C_2(\Delta)$, cf. eq 5, was calculated for a vector from the calcium ion to the oxygen of its water ligands. The corresponding correlation time, $\tau_{2,lig}$, was 1.9 ps and is probably mainly determined by diffusion of liganded water molecules within the hydration shell. The preferred direction of the dipole vectors of liganded water molecules is manifested also in intramolecular correlation times. The τ_2 of the dipole vectors is 1.7 ps (n_1, see Figure 3) and thus nearly equals $\tau_{2,lig}$. On the other hand, τ_2 for n_2 and n_3 amount to 1.0 and 0.6 ps, respectively, and are thus comparable to the values for bulk water molecules, cf. Table V.

During the trajectory five ligand exchanges occur, which correspond to a mean ligand residence time, τ_M, of ≈50–60 ps, where τ_M is defined as the mean time a particular water molecule lives in the complex before changing place with a water molecule outside it. This number is very uncertain for statistical reasons and is larger than those obtained for some monovalent ions from MD simulations on electrolytes using the MCY water potential.[39] One author[6] gives an upper limit of 10 ps for the residence time at normal pressure (≈1 bar). For the ligand exchanges in our trajectory, the departing ligand leaves before the arriving one is inserted, in four cases out of five. Thus, a large pressure would seemingly induce an increase in residence time, which may be the cause of the simulation value of τ_M, as the pressure was ≈2000 bar.

EDTA Simulations Performed. Two simulations of CaEDTA in water were performed. One used crystal coordinates of Ca(CaEDTA)·7H_2O as starting coordinates.[8] One of the two calcium ions occupies the EDTA binding site and has only two water ligands. The coordinates of these four molecules were used, and the remaining calcium ion and five water molecules were discarded. This complex was immersed in a further 312 water molecules in a cubic box with a side length of 21.7 Å. The water molecules, the orientations of which were randomized, were placed on the bases of a primitive cubic lattice, except for the volume occupied by EDTA. Below, this simulation will be referred to as the "C" simulation. Following on this, the Ca^{2+} ion was removed, and the four carboxyl groups were covalently protonated, which corresponds to a low pH value. The system was then left to reequilibrate, whereafter a further trajectory was recorded. This will be referred to as the "H" simulation in the following.

The second simulation was performed to obtain a check on equilibration times and on the sensitivity to starting configuration. As initial configuration, the coordinates of $MgEDTA^{2-}$ and those of the single magnesium liganded water molecule from the crystal coordinates[9] of Mg(MgEDTA)·9H_2O were used. The Mg^{2+} was replaced by a Ca^{2+}, and 316 water molecules were added. The simulation will be referred to as the "M" simulation. Parameters for the three trajectories are given in Table IV.

Thermodynamic averages for these simulations are given in Table IV. The difference in potential energy between the "H" simulation on one hand and the "C" and "M" simulations on the other is of course due to the absence of the strong calcium–ligand electrostatic interactions in the "H" case. Using the EDTA crystal coordinates one obtains that the electrostatic energy of $CaEDTA^{2-}$ is lower than that of H_4EDTA by ≈2500 kJ/mol. This figure is comparable to the simulation results.

Structural Properties of EDTA. In no case ("C" or "M") is the calcium ion released from the complex. However, we do observe changes in ligandation. In the "C" trajectory one carboxyl ligand is released, and in two of the other carboxyl groups, ligandation is transferred from one oxygen atom to the other. One water ligand is added. In the "M" trajectory, one carboxyl group turns to make both oxygen atoms interact strongly with the calcium. One water ligand is added, and the original water ligand is exchanged.

Radial distribution functions for the carboxyl oxygen atoms, the nitrogen atoms, and the water oxygen atoms, all with respect to the calcium ion, are plotted in Figure 6 for the "M" simulation. The corresponding functions for the "C" case are very similar,

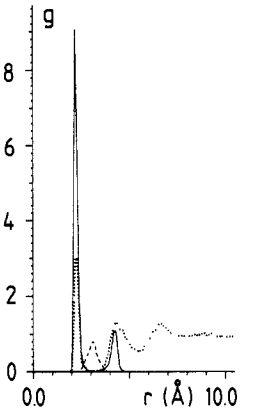

Figure 6. Radial distribution functions for the distances between the calcium ion and three different sets of atoms obtained from the "M" simulation. The first set contains the eight EDTA oxygen atoms (solid line), the second set contains the two EDTA nitrogen atoms (dashed line), and the third set contains all water oxygens (dotted line).

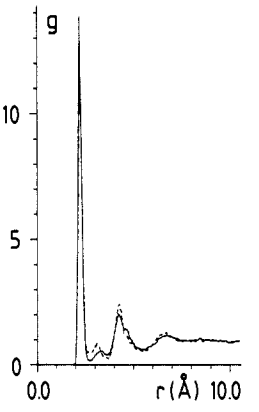

Figure 7. Radial distribution function obtained as the sum of the three radial distribution functions of Figure 6. The solid line represents the function obtained from the "C" simulation and the dashed line that obtained from the "M" trajectory.

as indicated by Figure 7 (see below), except for the occurrence of distances larger than 4 Å in the "Ca^{2+} to EDTA oxygens" function. This is a consequence of the above-mentioned carboxyl ligand release. In both the "C" and the "M" trajectories the two nitrogen atoms slightly recede from the calcium ion, to a distance of 3.2 ± 0.3 Å, and in the "C" case, where one carboxyl ligand was released, even farther away. The carboxyl ligands remain much closer to the calcium ion, i.e., at an average distance of 2.3 ± 0.1 Å. The integral of the first peak amounts to ≈4.6 oxygen atoms, and the remaining ≈3.4 are not liganded to the calcium ion (average distance 4.2 Å). The interaction between carboxyl groups and their spatial neighbors reduces the average carboxyl O–C–O angle from its vacuum equilibrium value of 129° to ≈121° ± 5°, whereas the average C–O bond length is not significantly altered. The first moment of the carboxyl group charge distribution thereby increases by ≈14%. For the relatively few cases were both oxygens ligand the calcium ion, the angle is reduced to 116° ± 5°, further increasing the polarity of the group. Three peaks are well-resolved in the water oxygen radial distribution functions. The nearest-neighbor peak, which contains the liganded water molecules, is situated at 2.3 ± 0.1 Å and amounts to ≈2.0 water molecules (this number increases to about 3 when, in the "C" trajectory, one carboxyl ligand has been released). The next peak is centered at 4.3 ± 0.5 Å and contains about 13–16 water molecules. This shell consists of the water molecules that are hydrogen bonded to the actual calcium ligands but is also partly due to the general shape of the EDTA complex. There is also a third, weakly pronounced water shell at ≈6.6 Å, whereas outside ≈7.5 Å the constant bulk water density prevails.

The sum of these three radial distributions is plotted in Figure 7 for the "C" and "M" simulations. The similarity of the two

(39) Impey, R. W.; Madden, P.; McDonald, I. R. *J. Phys. Chem.* **1983**, *87*, 5071–5083.

Table VI. Comparison of Configurations by Means of R Factors (eq 8)[a]

	XM	C_{bef}	C_{aft}	M	H
XC	1.36	1.1 ± 0.3	2.1 ± 0.2	1.2 ± 0.3	2.0 ± 0.2
XM		0.9 ± 0.2	1.6 ± 0.2	0.8 ± 0.2	1.5 ± 0.2
C_{bef}				0.9 ± 0.2	1.4 ± 0.4
C_{aft}				1.6 ± 0.3	1.3 ± 0.3
M					1.4 ± 0.3

[a] All R factors are given in Å. The designations XC, XM, C_{bef}, C_{aft}, M, and H refer to sets of configurations and are defined in text. For $R(a,b)$ values where a or b refers to a trajectory, the given values have been averaged over equidistant points, with a spacing of 0.96 ps, from the trajectory concerned. Where both a and b refer to trajectories, R has been averaged over both but with a spacing between points of 3.84 ps.

functions is obvious. All candidates for calcium ligandation are comprised in this "total" rdf, thus the number of ligands can be obtained from its integral. Conclusion of the integration at 2.7 Å gives a coordination number of ≈6.7, whereas extending the integration to 3.5 Å will include the two nitrogen atoms to make a total of ≈8.4 ligands. Note that in the Mg(MgEDTA)·$9H_2O$ crystal complex the central Mg^{2+} ion (replaced by a Ca^{2+} in simulation) is heptacoordinated, whereas in the crystal Ca(CaEDTA)·$7H_2O$ the central ion possesses eight ligands. In comparison, a luminescence study[40] of $EuEDTA^-$ and $TbEDTA^-$ in aqueous solution showed that Eu^{3+} and Tb^{3+} in these complexes have about three water ligands. As europium and terbium normally have slightly larger coordination numbers than calcium, this finding is consistent with our simulation results on $CaEDTA^{2-}$.

Comparison of the general structure of the $CaEDTA^{2-}$ complex in different environments was achieved by means of R factors, as applied in the refinement of X-ray crystallography data.[41] The R factor for a pair of configurations a and b, denoted by $R(a,b)$, was taken to be the minimum of the function R of eq 10

$$R = [\sum_{i=1}^{N} m_i|r_{i,a} - r_{i,b}|^2 / \sum_{i=1}^{N} m_i]^{0.5} \qquad (10)$$

where m_i is the mass of atom i and $r_{i,a}$ and $r_{i,b}$ its position in the two configurations. The summation covers Ca^{2+} and the atoms of $EDTA^{4-}$, in all 33 atoms, except for where one of the configurations is taken from the "H" simulation, when the R factor was calculated on the basis of the 32 $EDTA^{4-}$ atoms. Minimization is performed with respect to interconfigurational position and orientation. The R factor provides a comprehensive, quantitative measure of the similarity of configurations. Further, the minimization of R provides the translation and rotation for optimal superposition and thus the basis of any comparison of specific parts of the structure. To obtain an indication of the upper limit of R factors, the EDTA configuration at the starting point of the "M" simulation was taken, and an entire half of the molecule was rotated 180° around the C–C bond of the central ethylene, cf. Figure 1. The R factor between this configuration and the one before rotation was evaluated and found to be 2.32 Å. This value is thus to be considered very large for EDTA.

Some R factors are shown in Table VI. We will use the following notation to facilitate the discussion. Let XM denote the MgEDTA crystal coordinate set, XC the CaEDTA crystal coordinate set, C_{bef} a configuration from the "C" trajectory taken before the release of the carboxyl ligand, C_{aft} one taken after that release, and M and H configurations from the "M" and "H" trajectories, respectively. We note that $R(C_{bef},XC) \approx R(M,XC)$ and that $R(C_{bef}, XM) \approx R(M,XM)$. Further, both trajectories display $CaEDTA^{2-}$ configurations that on the average are

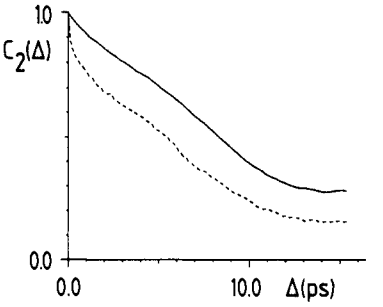

Figure 8. Second-order time correlation functions, $C_2(\Delta)$, obtained from the "M" trajectory. $C_2(\Delta)$ for the EDTA nitrogen–nitrogen vector (solid line) and for the eight EDTA acetic acid C–H vectors (dashed line) is shown.

somewhat closer to the crystal $MgEDTA^{2-}$ structure. This is most likely due to the fact that the second metal ion is in part liganded directly to the EDTA molecule in the Ca(CaEDTA)·$7H_2O$ crystal and thus distorts it, which is not the case for the Mg(MgEDTA)·$9H_2O$ crystal. This is also reflected by R(XC, XM) being as much as 1.36 Å. $R(C_{bef}, M)$ approximately equals $R(C_{bef}, XM)$ and R(M, XM), while $R(C_{aft}, M)$ is close to $R(C_{aft}, XM)$. However, $R(C_{bef}, M)$ features some very low minima, the lowest of which is 0.33 Å, indicating very similar conformations. Thus there is at least one area of configurational space, that both trajectories have traversed, albeit originating from very different starting points (R(XC,XM) = 1.36 Å). For the "H" trajectory, we note that R(H,d) is not larger than $R(C_{aft},d)$, where d belongs to the set D = {XC, XM, M}, i.e., that the "H" configurations do not deviate more from the configurations of set D than do the configurations where one EDTA calcium ligand has been replaced by water. We may reword that as follows. If we take XM or M as a reference set, we find that the configurations where a water molecule has supplanted a carboxyl ligand, forcing the latter outwards, are deformed to about the same extent as those where the four carboxyl groups may move freely. Note also that the carboxyl groups each have a hydrogen in the "M" case and thus do not repel each other electrostatically. On the other hand, R(H,b) is significantly larger than $R(a,b)$, where a and b belong to the set A = {XC, XM, C_{bef}, M}, thus "H" configurations deviate more from all configurations of set A than any from that set deviates from any other. In addition, no configuration pairs H,C_{bef} nor H,M could be found possessing an R factor below 0.83 Å, which is very much larger than the minima for C_{bef},M. In other words, there is no H configuration that resembles any C_{bef} configuration, and none that resembles any M configuration. We conclude that the simulations very clearly distinguish between the EDTA where the calcium ion is present, and that where it is not.

The similarities between the "M" and "C" trajectories discussed here and above indicate that the structural properties of the system are determined by the potential and the macroscopic parameters, i.e., that the system is quasiergodic, and also that an equilibration time of ≈17 ps is adequate for this kind of system.

Dynamic Properties of EDTA. First- and second-order reorientational correlation functions (cf. eq 5) were calculated for a set of vectors of the $CaEDTA^{2-}$ complex. Two of these are shown in Figure 8. First estimates of the corresponding correlation times were obtained by fitting an exponential between 0.5 ps and 6.0 ps to the tcf's. For such an estimate to be accurate, it is necessary that the length of the simulation be several times larger than the estimate itself, which is not the case here. Moreover, the tcf's themselves possess but little resemblance to singly exponential functions, and in consequence the general definition of the correlation time as the integral of the correlation function (normalized so as to make C(0) = 1) is to be preferred. The use of this definition is also prerequisite of any comparison to NMR data. Straightforward evaluation of that integral is not possible, however, as the tcf's are available only up to some time Δ_L, and their tail for times larger than that normally contributes considerably to the integral. In principle, Δ_L equals the length of the trajectory, T_L, but the statistic uncertainty is acceptably small

(40) Horrocks, W. DeW.; Sudnick, D. R. *Acc. Chem. Res.* **1981**, *14*, 384–392.

(41) See, for instance: Cantor, C. R.; Schimmel, P. R. *Biophysical Chemistry, Part II: Techniques for the Study of Biological Structure and Function*; Freeman: San Francisco, 1980; pp 763–788. The procedure followed here corresponds to eq 13–108 of that ref, but in real space and with $\kappa = 1$ and W_{hkl} equal to the relative masses of the atoms.

Table VII. Dynamic Properties of EDTA[a]

		"C"	"M"	"H"	exprmnt
C–H	τ_1	26 ± 5	28 ± 4	14	
		15 – 38	19 – 41		
	τ_2	7 ± 1	8 ± 1	4	58
		5 – 10	7 – 11		
N–N	τ_1	42 ± 3	45 ± 6	15	
	τ_2	13 ± 1	14 ± 2	6	
"overall"	τ_1	49 ± 4	47 ± 9		
	τ_2	15 ± 1	15 ± 2		
diffusion coeff		1.0	1.1	2	0.59
		(0.8 – 1.6)	(0.4 – 2.4)		

[a] Correlation times are given in ps, diffusion coefficients in 10^{-9} m^2/s. The "overall" values were obtained from the sum of the correlation functions of the EDTA Ca–N′, the Ca–N″, and the N′–N″ vectors. The uncertainty for the diffusion coefficients is given as the range of values obtained for different parts of the trajectory. The experimental correlation time is taken from ref 11 and the experimental diffusion coefficient from ref 10. Experimental data apply to $CaEDTA^{2-}$.

only at times $\Delta \ll T_L$, and thus $\Delta_L \ll T_L$. To circumvent this difficulty one may approximate the tail of the correlation function by $C(\Delta_L)\exp[-(\Delta-\Delta_L)/\tau]$. Then

$$\tau = \int_0^\infty C(\Delta)\,d\Delta = \int_0^{\Delta_L} C(\Delta)\,d\Delta + \int_{\Delta_L}^\infty C(\Delta_L)\exp[-(\Delta-\Delta_L)/\tau]d\Delta = I + \tau C(\Delta_L)$$

$$\tau = I/[1 - C(\Delta_L)] \qquad (11)$$

where I is the (numerically evaluated) integral of $C(\Delta)$ from 0 to Δ_L. If $C(\Delta)$ contains a well discernible and rapidly decaying component ($\tau_f \ll \Delta_L$) this may be taken into account. Take $C(\Delta) = AC_f(\Delta) + BC_s(\Delta)$ with $A + B = 1$, and A and B known. Then $\tau = A\tau_f + B\tau_s$. Now, if $A\tau_f \ll \tau$ one obtains

$$\tau = \int_0^{\Delta_L} C(\Delta)\,d\Delta + \int_{\Delta_L}^\infty C(\Delta_L)\exp[-(\Delta - \Delta_L)/\tau_s]d\Delta \approx I + \tau C(\Delta_L)/B$$

$$\tau = BI/B - C(\Delta_L) \qquad (12)$$

Correlation times were obtained from eq 12 and are given in Table VII. For the C–H vectors the average tcf for all eight vectors was analyzed. The uncertainties in the correlation times are the standard deviation in averaging the different correlation times obtained as a result of using different values of Δ_L, evenly distributed from 3 to 24 ps. These uncertainties are very much less than the range of correlation times obtained for individual methylene groups also given in Table VII. For reasons of symmetry, all four acetic acid methylenes should have the same correlation times but only in the limit $T_L \to \infty$, a condition which is obviously not fulfilled in these simulations. Given in Table VII is also an experimental value of the C–H second-order correlation time as obtained by ^{13}C NMR.[11] The ratio to the simulation value is about 7.

The mean-square displacement of the EDTA complex center of mass was calculated as a function of time, from which the diffusion coefficient was obtained, cf. Table VII. From experimental data, Mateo et al.[10] give a value of $\approx 0.59 \cdot 10^{-9}$ m^2/s at 303 K, which is about half the simulation value.

Discussion of EDTA Properties. There are several difficulties in simulations of large molecular systems, particularly as regards comparison to experiment. One such is the intermolecular potential which here, as in most other simulations reported, has been assumed to be pairwise additive. This is obviously an approximation, especially for charged systems, which partly can be remedied by using an effective pair potential, which includes the nonadditive terms in an average way. It is however very difficult to assess the accuracy of this approximation. Thus we cannot a priori expect MD simulations to achieve full reproduction of physical properties. The strong interaction of the calcium ion and the nitrogen atoms of the EDTA molecule in the crystal structures is mostly due to the nitrogen lone pair of electrons, which is strongly polarized by the electric field of the calcium ion. We interpret the weak ligandation of the nitrogen atoms in the simulations to be caused by the absence of this term in the potential. Concomitant to this partial neglect of the inductive term in the calcium–nitrogen relation is an increase in internal mobility.

Also the carboxyl groups will be polarized by the calcium ion, and the effective charge transfer across the carboxyl group will be significant. A charge transfer of 0.1 e amounts to a decrease in potential energy of ≈60 kJ/mol per carboxyl group. The polarization will strengthen the ligandation of the carboxyl group as a whole. As the polarizability of the carboxyl group is larger in the direction from one oxygen atom to the other, the polarization will also increase the energy barrier for rotation of that group. From the energies involved, this increase in barrier height will decrease the probability of carboxyl flips and even more so the probability of a carboxyl ligand release, by several orders of magnitude, and they might be entirely inhibited on the time scales accessible to MD simulation. This line of reasoning is consistent with the very low rate constant found for the dissociation of Ca^{2+} from EDTA.[42] The observed carboxyl flips (two in the "C" trajectory, one in the "M" trajectory) and the carboxyl group release ("C" trajectory) certainly entail increased motion in adjacent parts of the complex. This internal motion is substantiated by the correlation times being shorter for the acetic acid C–H vectors than for the N–N and Ca–N vectors, where the tcf's of the latter may be assumed to represent reorientation of the entire complex.

There is some evidence in the literature that EDTA chelates calcium in two forms, either hexadentately or pentadentately.[43] In the latter case one carboxyl oxygen ligand has been replaced by a water molecule, as occured in the "C" trajectory. The experiments were however interpreted on the assumption that Ca^{2+} has a coordination number of 6, and it is not clear to us whether a larger coordination number would affect this interpretation or not.

The presence of internal motion leads to a partial breakdown of the hydrodynamic model. While the diffusion coefficient more or less monitors the bodily size of the $CaEDTA^{2-}$ complex, the reduction in correlation times caused by intramolecular flexibility precludes consistency within the model as formulated by eq 7. From the simulation value of the water viscosity, the EDTA diffusion coefficient and second-order reorientational correlation time, eq 7 yield $r_{e,D} = 7.4$ and $r_{e,\tau} = 3.8$ Å, values that differ by nearly a factor of 2. In comparison, the volumes of the crystal Ca^{2+} and Mg^{2+} complexes correspond to effective radii of 5.9 and 5.7 Å, respectively. The failure of the hydrodynamic model may not apply to real $CaEDTA^{2-}$; however, since tightening up the structure would result in longer correlation times. Also, with the internal motions much more restricted the correlation times of any intramolecular vector, such as the methylene C–H vectors, would more or less equal those of the overall reorientation, cf. Table VII.

The motion of the $CaEDTA^{2-}$ complex as a whole is determined by the solvent, i.e., by the dynamic properties of water itself. Comparison of experimental and simulation data on water dynamics can be used to correct the simulation results on the dynamic properties of EDTA. The simulation overall rotational correlation time, τ_2, for $CaEDTA^{2-}$ multiplied by the ratio between experimental and simulation values for the water rotational correlation time or diffusion coefficient gives ≈39 ps. On assumption of the hydrodynamic model, we may instead multiply by the ratio between experimental and simulation water viscosities, to give a result of ≈52 ps. These considerations in conjunction with the assumption of restricted internal mobility would also account for the discrepancy between the simulation and NMR values of the acetic acid C–H vector correlation times.

(42) NMR data, such as those in ref 11 yield $k_{off} < 10\ s^{-1}$.
(43) Harada, S.; Funaki, Y.; Yasunaga, T. *J. Am. Chem. Soc.* **1980**, *102*, 136–139.

Conclusion

From the data presented in this work we conclude that quasiergodicity is reached relatively quickly and that the used equilibration times are adequate. For bulk water and the solvated calcium ion, static properties seem to be plausibly represented by the present potential, as are also qualitatively dynamic properties. The failure to quantitatively reproduce dynamic, experimental data is mainly due to the absence of dynamic data in constructing the intermolecular potential. A water model that allows for intramolecular motion while correctly reproducing dynamic properties is desirable but lacking. Also for the larger EDTA molecule, structural properties are qualitatively reproduced but are more sensitive to the imperfections of the potential. The binding of the calcium ion to EDTA is adequately treated in most respects. The $CaEDTA^{2-}$ overall mobility is too large, but this may be corrected for by use of the known properties of the water model and experimental data. While shortcomings of the intramolecular EDTA potential render the simulation dynamics locally incorrect, the mechanism of this seems well understood and can be taken into account in the interpretation of simulations. We think the present simulations contribute substantially to the understanding of calcium binding, which; in view of its biological importance, certainly merits further investigation.

Acknowledgment is due to Bo Jönsson for valuable discussion and to The Swedish Natural Science Research Council for financial support (Grant no. K-KU 4356-104).

Registry No. Ca, 7440-70-2; H_2O, 7732-18-5; EDTA, 60-00-4.

Calculated Structures and Fluoride Affinities for Fluorides

M. O'Keeffe

Contribution from the Department of Chemistry, Arizona State University, Tempe, Arizona 85287. *Received September 30, 1985*

Abstract: It is shown that SCF–MO calculations provide good estimates of the energies of the processes $MF_n \rightarrow M^{n+} + nF^-$ where M^{n+} is an ion of a first- or second-row element in a closed-shell or s^2 configuration. The fluoride ion affinities are then calculated for a number of molecules and ions. Where comparison with experiment is possible, the agreement is generally good when allowance is made for experimental uncertainties. In favorable cases, accurate heats of formation may be calculated from fluoride affinities.

Fluoride ion affinities of molecules and ions are of considerable theoretical and experimental interest. Experimental values come mainly from ion cyclotron resonance (ICR) experiments[1-3] or from Born–Haber (BH) thermodynamic cycles.[4,5] Most of the derived results are indirect, and it is often quite difficult to assess uncertainties reliably. It is important therefore to have an independent set of fluoride affinities to compare with experimental values and to provide estimates of values as yet not determined.

In this work it is shown that ab initio SCF–MO calculations can provide reliable fluoride affinities, at least in certain instances. The important point about such calculations is that they should be made only for processes in which there is no change in multiplicity and ideally for singlet state species.[6] Previous calculations of the fluoride affinity of HF[7,8] and of H_2O[9] have shown that in these cases at least the change of correlation energy is only a small fraction of the energy change and less than experimental error, which is typically >5 kJ mol^{-1}.

Methods

Equilibrium geometries and SCF energies have been calculated for a number of first- and second-row fluoride molecules and ions in singlet states. The 6-31G* basis set[10] was chosen as a reasonable compromise between the desire, on the one hand, to have a sufficiently flexible basis set to predict geometries reliably and to avoid basis set superposition errors and, on the other hand, to allow reasonably heavy molecules to be studied without untoward cost. It is well-known[11] that for negative ions (F^-, etc.) additional diffuse valence orbitals are necessary, so the F basis was supplemented

Table I. Energy (kJ mol^{-1}) for $MF_n \rightarrow M^{n+} + nF^-$

MF_n	expt[a]	theor	ratio[b]
HF	1573	1591	0.989
LiF	772	764	1.011
BeF_2	3285	3273	1.004
BF	1241	1196	1.038
BF_3	7859	7800	1.008
CF_2[c]	3848	3762	1.023
CF_4	14949	14775	1.012
NF_3	8700	8510	1.022
NaF	650	635	1.024
MgF_2	2564	2533	1.012
AlF	913	906	1.008
AlF_3	5931	5869	1.011
SiF_2	2943	2866	1.027
SiF_4	11036	10863	1.016
PF_3	6369	6191	1.029
PF_5	17789	17421	1.021
SF_4	11272	10917	1.033
SF_6	26701	26161	1.021

[a] Data from ref 13 except electron affinity of F from ref 14 and zero point energies estimated from frequencies given in ref 15. [b] Expt/theor. [c] Heat of formation from ref 15.

(1) Larsen, J. W. McMahon, T. B. *J. Am. Chem. Soc.* (a) **1985**, *107*, 766; (b) **1983**, *105*, 2944; (c) **1982**, *104*, 5848.
(2) Murphy, M. K.; Beauchamp, J. L. *J. Am. Chem. Soc.* **1977**, *99*, 4992.
(3) Haartz, J. C.; McDaniel, D. H. *J. Am. Chem. Soc.* 1973, *95*, 8562.
(4) Altshuller, A. P. *J. Am. Chem. Soc.* **1955**, *77*, 6187.
(5) Mallouk, T. E.; Rosenthal, G. L.; Müller, G.; Brusasco, R.; Bartlett, N. *Inorg. Chem.* **1984**, *23*, 3167.
(6) Hurley, A. C. *Adv. Quantum Chem.* **1973**, *7*, 315.
(7) Noble, P. N.; Kortzeborn, R. N. *J. Chem. Phys.* **1970**, *52*, 5375.
(8) Emsley, T.; Parker, R. J.; Overill, R. E. *J. Chem. Soc. Faraday Trans. 2* **1983**, *79*, 1347 and references therein.
(9) Kistenmacher, H.; Popkie, H.; Clementi, E. *J. Chem. Phys.* **1973**, *59*, 5842.
(10) Pietro, W. J.; Hehre, W. H.; Binkley, J. S.; Gordon, M. S.; DeFrees, D. J.; Pople, J. A. *J. Chem. Phys.* **1982**, *77*, 3654 and references therein.
(11) Dunning, T. H.; Hay, P. J. In *Modern Theoretical Chemistry*; Schaeffer, H. F., Ed.; Plenum Press: New York, 1977.

0002-7863/86/1508-4341$01.50/0